Macromolecules

ARTICLE

pubs.acs.org/Macromolecules

Universality and Percolation in Biodegradable Poly(ε-caprolactone)/Multiwalled Carbon Nanotube Nanocomposites from Broad Band Alternating and Direct Current Conductivity at Various Temperatures

Alfredo Bello,[†] Estrella Laredo,*[,†] Jesús R. Marval,[†] Mario Grimau,[‡] María L. Arnal,[‡] and Alejandro J. Müller[‡]

[†]Departamento de Física and [‡]Departamento de Ciencia de los Materiales, Universidad Simón Bolívar, Apartado 89000, Caracas 1080, Venezuela

Benoit Ruelle and Philippe Dubois

Center of Research and Innovation in Materials and Polymers CIRMAP, Service des Matériaux Polymères et Composites SMPC, Université de Mons-UMONS, Place du Parc 20, B-7000 Mons, Belgium

ABSTRACT: Dc and ac conductivities in a broad angular frequency, $2\pi \times 10^{-3}\ s^{-1} < \omega < 2\pi \times 10^{7}\ s^{-1}$, and temperature range, 133 K < T < 323 K, were measured in poly(ε-caprolactone)/multiwalled carbon nanotube nanocomposites as a function of weight concentration (0 wt % ≤ p ≤ 3 wt %). The universal dynamic response was observed at low p values, and the parameters were adjusted by working in several domains. Scaling laws predicted by the variation of dc conductivity as a function of p or characteristic frequency in percolation theory were followed and showed the formation of a 3D percolative cluster at concentration values as low as 0.3 wt %. The existence of tunneling conduction was proved, and its independence on temperature indicates that we are in the presence of a conventional tunnel effect among nanoparticles not yet in physical contact, through energy barriers made by the polymer chains. All these combined facts allowed construction of a master curve evidencing the time−temperature−composition superposition existing in the poly(ε-caprolactone)/multiwalled carbon nanotube nanocomposites studied here.

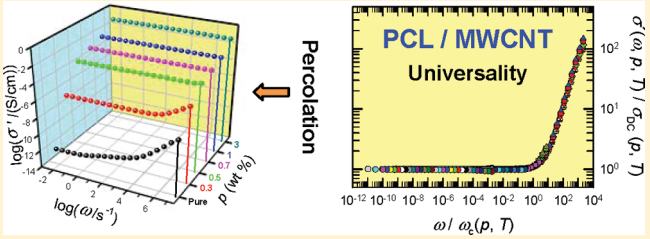

1. INTRODUCTION

The applications of materials reinforced with carbon nanotubes (CNT) take advantage of the novel properties of these nanobjects that in low concentration, if they are well dispersed, may enhance and modify the mechanical, electric, dielectric, thermal, and crystallization properties of the host material or even induce new nanoeffects.[1] The CNT present interesting transport properties that modify the insulator characteristics of the polymer matrix where they are included. CNT, being 1D, may form an infinite cluster, which allows percolation of charge carriers in a nonconductive matrix at low concentrations; also, tunneling-assisted conductivity through the thin barrier that separates them at low concentrations contributes to the rise of several decades in the dc conductivity, even if physical contact is not yet achieved. The blending of polymer matrices with well-dispersed CNT as the filler (less than 5% in weight) results in drastic improvements in the properties of the neat material, such as better processability and mechanical and electric properties, without any drawback due to their light weight. Many applications such as organic LEDS,[2] fuel cell membranes, photovoltaic devices,[3,4] and chemical sensors and actuators[5] have been realized.

The success of a given nanocomposite is due to the achievement of a good dispersion of the nanofiller in the polymer matrix. This is sometimes difficult to obtain and many approaches have been taken to overcome the lack of chemical compatibility in order to increase the affinity of the CNT to the macromolecular chains; also, the tendency for CNT agglomeration due to their van der Waals interactions favors the bundle formation. The challenge of determining the CNT distribution in a polymer matrix demands the use of a combination of morphological characterization techniques.[6] An alternative measure of the dispersion of the nanofiller in the polymer matrix is given by the conductivity percolation threshold, which might be expressed as the CNT weight percent concentration, p_c, which is necessary to observe a steep increase in the dc conductivity. This is the manifestation of the existence of a continuous path for the charge carriers through the sample. The dispersion of the CNT is the result of a combination of parameters such as CNT type [single-walled carbon nanotubes (SWCNT) always show lower p_c than multiwalled carbon nanotubes (MWCNT)], synthesis or blending methods, thermal treatments, chemical functionalization,[7] CNT aspect ratio L/R, (L being the length and R the outer radius), and the chosen polymer matrix, which can be either

Received: November 15, 2010
Revised: March 1, 2011
Published: March 25, 2011

amorphous or semicrystalline.[8] The amorphous phase which hosts the CNT also changes from a glassy to a rubbery state as temperature increases. Additionally, the often found nucleating effect of the CNT leads to lamellae growth in the CNT vicinity. Bauhofer and Kovacs[9] have gathered published data on 30 polymers loaded with CNT. The analysis of the 147 experimental results, which included p_c, the critical exponent t, and the maximal conductivity, lead them to conclude on the importance of the type of polymer and dispersion method. For PE in its different densities, the percolation threshold varied from 0.045 to 15 wt % while the critical exponent varied from 15 to 1.8. No correlation was found among these two parameters. Extreme values, t = 8.4 in polyamide-6/MWCNT composites, have also been recently reported and attributed to a predominant tunnel conduction among nanotubes with a wide distribution in the interparticle distance, i.e., in the potential barrier thickness.[10]

Poly(ε-caprolactone) (PCL) is an aliphatic semicrystalline polyester that is biodegradable and biocompatible with many potential uses in medicine, such as controlled drug release, and in tissue engineering, as temporary scaffolds for tissue growth. The properties of PCL need to be improved for some applications, and several approaches have been taken: (a) blend[11,12] or copolymerize[13] the PCL with other biopolymers such as polylactide (PLA), (b) reinforce the PCL resin with nanofillers such as nanoclay[14] or CNT,[15−17] and (c) blend and reinforce the mixture with CNT as in PCL/PLA/CNT ternary nanocomposites.[18,19]

The well-dispersed SWCNT in the PCL/SWCNT nanocomposites studied by Mitchell and Krishnamoorti[16] showed, after dc measurements, a very low electrical percolation threshold, p_c = 0.08 wt %, when a zwitterionic surfactant was used in the preparation of the materials. The geometric percolation value, obtained after melt rheological experiments, also lead to the same low value for the percolation threshold. Another consequence of the SWCNT introduction in the PCL matrix is the large nucleating effect of the nanofiller, as shown by differential scanning calorimetry (DSC)[15] and combined DSC and X-ray diffraction at wide angle (WAXS) and small angle (SAXS) techniques.[20] The nucleating effect is evidenced by the remarkable acceleration of the PCL crystallization rate and the increase in crystallization temperature without significant changes either in the melting temperature or in the crystallinity degree.

We have previously studied the electrical and dielectric properties of PCL/PLA/MWCNT ternary nanocomposites, the MWCNT being functionalized with −COOH groups and selectively located on the inclusions interface of the sea-island morphology of the immiscible blend.[19] The CNT concentration necessary to observe percolation was 1 wt % for the blend nanocomposites. It is to be noted that two recent compilations on CNT/polymer composites by Bauhofer and Kovacs[9] and Spitalsky et al.[21] only mention two previous works[16,22] on PCL/CNT, which only report dc conductivity results at room temperature as they focused on other properties of the nanocomposites.

The broad band dielectric spectroscopy, BBDS, is the best tool to study the nanocomposite's electrical properties, as its results can be represented in dielectric constant, conductivity, or electric modulus domain in the broad frequency and temperature ranges that are now available. The variation of the electrical properties of nanocomposites based on different homopolymers such as polycarbonate,[23] polyethylene,[24] and polyepoxy[25] filled with MWCNT have been intensively studied, while no previous report has been found on neat PCL. The drastic variation of the conductivity when the percolative CNT network is formed allows one to determine the percolation parameters, such as the threshold concentration (p_c), the critical exponent for the conductivity (t), and the critical frequency (ω_c).[26] Also, the contribution of tunneling through thin barriers has been detected.

The purpose of this work is to study the effect of the introduction of pristine CNT in PCL matrix on the dielectric and electrical properties as a function of CNT concentration, temperature, and frequency, below and above the percolation threshold. Nanocomposites based on this important biodegradable homopolymer have not been previously studied by these techniques. The results obtained by us on the 70/30 PCL/PLA blend might not be extrapolated to the PCL homopolymer due to the particular location and carboxylic functionalization of the CNT.[19] Here, the experiments were carried out over a wide temperature range that covers glassy and rubbery state, which is not very frequent in nanocomposites BBDS studies. The results will be presented in different domains, i.e., conductivity, permittivity, and electric modulus, in order to obtain the best parameters of the universal dynamic response used in the modeling of the ionic or electronic conduction in disordered materials. Percolation theory will be applied in order to determine the characteristic parameters of the process, which are scarce in the literature as previous studies were focused on dc results. The universality of the ac conductivity will be tested through master curve construction. Parallel WAXS and calorimetric experiments will add information on the crystalline phase structure and its abundance, and the role of CNT as a nucleating agent for PCL will be studied. Comparison of the effect of CNT dispersed in PCL and CNT selectively located in the PCL phase of the biopolymers blend, PCL/PLA, will be presented.

2. EXPERIMENTAL SECTION

2.1. Materials. Poly(ε-caprolactone) was obtained from Solvay Interoxy Belgium (CAPA 6500, $M_n \sim 50\,000$ g/mol). MWCNT (NC 7000) were produced via catalytic carbon vapor deposition by Nanocyl S. A., Belgium. Their mean diameter was 9.5 nm and their average length 1.5 μm. MWCNT were dried mixed with the PCL homopolymer with a concentration of 3 wt % of MWCNT in the final material. The mixture with the chosen composition was introduced in the addition funnel of a Minilab twin-screw miniextruder equipped with corotating screws and a closed loop for recirculation set at 120 °C for 4 min at 30 rpm screw speed. This speed was increased to 60 rpm for 10 min, allowing the materials to circulate in the closed loop. The nanocomposites were recovered by opening the miniextruder, in order to avoid any preferred orientation of the CNT during the extrusion process. From this master batch, compositions equal to p = 0.3, 0.5, 0.7, 1, and 3 wt % were obtained. The samples were cut from compression-molded sheets at 100 °C and rapidly cooled in an ice−water mixture.

2.2. Wide-Angle X-ray Scattering. The existence of 3D order at room temperature was checked by WAXS. An X'pert-Pro Panalytical $\theta-\theta$ spectrometer was used. The X-ray wavelength was copper Ni-filtered Kα, λ = 1.541 78 Å.

2.3. Differential Scanning Calorimetry. Calorimetric studies to determine the crystallization and melting temperatures of the nanocomposites were carried out in a Perkin-Elmer Pyris 1 differential scanning calorimeter calibrated with indium and tin. Ultrahigh-purity nitrogen was used as a purge gas. Samples of approximately 5 mg each were encapsulated in aluminum pans and sealed. The crystalline thermal history was erased by heating the samples at 373 K for 3 min. Cooling

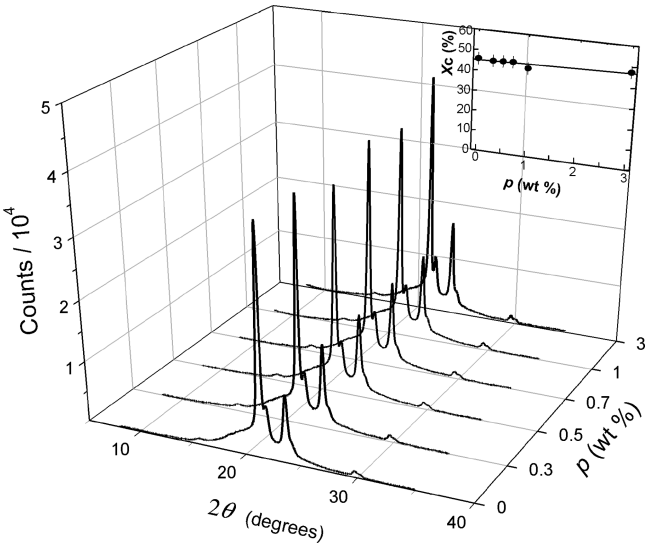

Figure 1. WAXS spectra of the nanocomposites PCL/MWCNT with different nanoadditives amounts. $\lambda_{Cu\,K\alpha}$ = 1.541 78 Å. The inset represents the variation of the PCL degree of crystallinity, X_c.

from 370 to 250 K and subsequent heating scans were registered at 20 K/min.

2.4. Ac Conductivity and Dielectric Experiments. An Alpha station by Novocontrol was used to record the conductivity spectrum at frequencies ranging from 10^{-3} to 10^{7} Hz. The ac applied voltage was 1 V rms. The isotherms varied from 133 to 313 K by 5 K steps; a flow of dry nitrogen gas regulated by a Quatro temperature control system by Novocontrol ensured a stability better than 0.1 K. The sample, with sputtered gold electrodes, was placed between gold-plated metallic electrodes in the cryostat, the contact being assured by a micrometer screw.

The data was collected as a function of frequency at each temperature, in the dielectric constant domain $[\varepsilon^*(\omega,T,p) = \varepsilon'(\omega,T,p) - i\varepsilon''(\omega,T,p)]$, the electric conductivity domain $[\sigma^*(\omega,T,p) = \sigma'(\omega,T,p) - i\sigma''(\omega,T,p)$, $\sigma' = \omega\varepsilon_0\varepsilon'']$, and the electric modulus domain $[M^*(\omega,T,p) = M'(\omega,T,p) + iM''(\omega,T,p)$, $M' = \varepsilon'/(\varepsilon'^2 + \varepsilon''^2)$, $M'' = \varepsilon''/(\varepsilon'^2 + \varepsilon''^2)]$.

3. RESULTS AND DISCUSSION

3.1. Crystallinity and Nucleating Effect. Crystallinity of nanocomposites was determined by WAXS experiments; in Figure 1 the spectra for all nanocomposites composition, $I(2\theta)$, are presented. The observed intense peaks with increasing θ are the Bragg reflections corresponding to (110), (111), and (200) planes of the orthorhombic unit cell (space group $P2_12_12_1$).[27] No alteration of the PCL crystal structure is observed. The crystallinity degree was calculated by deconvoluting each trace into the Bragg peaks and the contribution of the PCL amorphous zones. After subtracting a linear background, the curve is decomposed in eight narrow Pearson profiles with an average width of 0.36° originated by the crystal lamellae. The amorphous halo of PCL is a bimodal wide distribution made of two Pearson profiles with a large fwhm of about 4° in 2θ located at 2θ = 20.40° and 24.05°, these values representing the most frequent distances found in the disordered regions.

The crystallinity degree (X_c) is calculated as the ratio of the intensity diffracted by the crystalline zones to the total diffracted intensity in the 2θ range from 8 to 35°. The results, plotted as a function of p in the inset, show that there is no variation in the X_c values for 0% ≤ p ≤ 3%. The values found are almost identical and within 46% ± 1%. A similar result was found here after DSC experiments. Additionally, the crystallization (T_c) and melting (T_m) temperatures of the PCL crystallites in the nanocomposites were determined from the cooling traces, where a well-defined PCL crystallization exotherm was observed followed by the corresponding melting endotherm in the subsequent heating scan. Figure 2 summarizes the results obtained for the peak crystallization and melting temperatures when the MWCNT content was varied. A very important increase in the T_c value of PCL was observed, which corresponds to a dramatic increase in nucleation density commonly referred to as a nucleation effect. The T_c values jumped from 302 to 316 K, on going from p = 0% to 0.5%, indicating that the supercooling needed to crystallize the material was reduced by 14 K. This trend is commonly observed in the presence of nucleating agents,[28] where the increase in T_c is very steep at low loads and saturates above a specific concentration, which in the present case is remarkably low. However, for efficient nanofillers, as is the case here, the saturation occurs at very low concentrations. This has been recently reported for different types of PCL/CNT nanocomposites, showing the generality of this nucleating effect independent of the preparation of the composites.[15,29,30] In fact, the efficiency of the nucleation effect for our nanocomposites has been estimated to be extremely high as compared to the self-nucleation of PCL.[31,32] The values of the melting point are much less affected, as expected for metastable polymeric crystals, where a large increase in T_c is required to observe a small increase in T_m values. The mean X_c value found here is lower than that found for PCL in the ternary compounds, where, due to the exclusion from the PLA, the effective CNT concentration is higher and the nucleating effect is increased.[19]

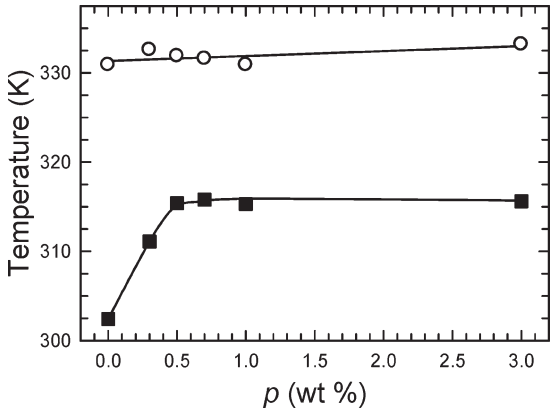

Figure 2. Variation of the peak crystallization and melting temperatures, T_c (■) and T_m (○), with nanofiller content for PCL/MWCNT nanocomposites. The lines are drawn to guide the eye.

3.2. Electrical Measurements. Several representations may be chosen to represent the ac data in different domains. In Figure 3 we have plotted, for all p values, the variation of the room temperature real part of the electric conductivity, $\sigma'(\omega)$ (Figure 3a), the dielectric losses, $\varepsilon''(\omega)$ (Figure 3b), and the imaginary part of the electric modulus, $M''(\omega)$ (Figure 3c). It is readily observed that the nanocomposites conductivity present a frequency-independent behavior at high p values accompanied by a steady decrease of $\varepsilon''(\omega)$ and monotonous increase in $M''(\omega)$ domain. Different frequency dependences are found for the less loaded PCL (0.3%) and the neat PCL. The increase of

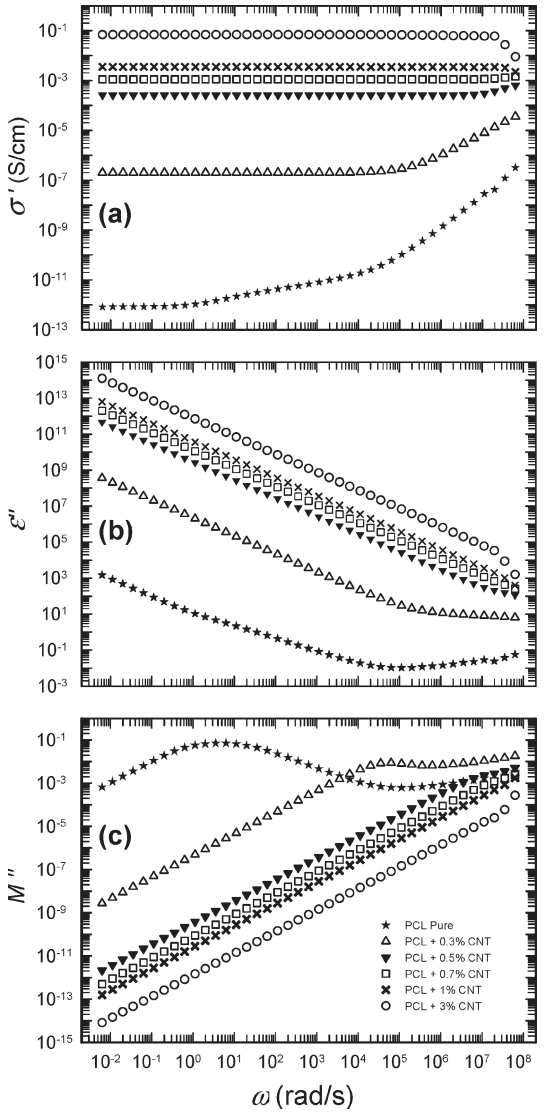

Figure 3. (a) Real part of the conductivity, (b) dielectric losses, and (c) imaginary part of the electric modulus, as a function of angular frequency, at room temperature, for the nanocomposites PCL/CNT with CNT wt % concentrations indicated in the legend.

the low frequencies conductivity is dramatic on going from p = 0% to 0.3% and 0.5%. The conductivity plateau value still increases as the nanofiller concentration grows for p > 0.5%. As our experiments at room temperature were carried out to very low frequencies, 10^{-3} Hz, the conductivity values recorded at these minimum frequencies were taken as $\sigma_{dc} = \sigma(\omega = 2\pi \times 10^{-3}\ s^{-1})$. Also there is a critical angular frequency, ω_c, which in our frequency window appears only at low p values, where the conductivity starts to increase after the lower frequency plateau. This critical frequency increases with p and its numerical value is taken, as usual, as the value where a 10% increase in the rising conductivity curve is observed, $\sigma(\omega_c) \approx 1.1\sigma_{dc}$.

In the absence of CNT, the precise analysis of the neat PCL conductivity curves (see Figure 4) shows the existence of relaxation processes in addition to the contribution of the dc conductivity at room temperature in the frequency window spanned here. The study of the dielectric response in neat PCL has been previously reported.[33] The results can be summarized in

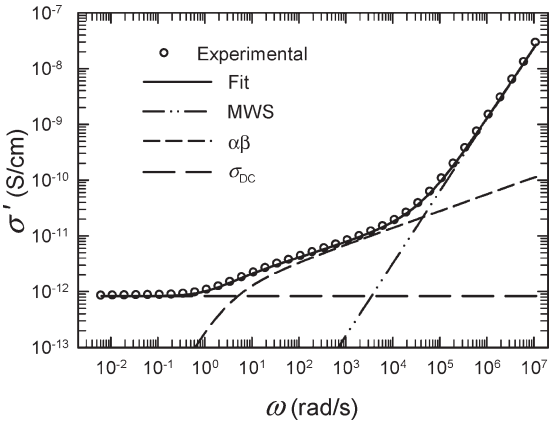

Figure 4. Example of analysis of the conductivity spectrum for neat PCL at room temperature.

the relaxation map, which represents the variation with the inverse of temperature of the Cole−Cole distributions mean relaxation times for each process used in the detailed analysis of the $\varepsilon''(\omega)$ isotherms.

Two modes were identified at room temperature in the broad frequency window used here: the lowest frequency mode is due to the relaxation of interfacial charge accumulation, or Maxwell−Wagner−Sillars polarization, while the highest frequency rise corresponds to the low frequency tail of the $\alpha\beta$ peak due to the merging of the segmental, α, and β processes (see Figure 9 in ref 33).

For the analysis of the p = 0.3 wt % nanocomposite conductivity, the contribution of the dielectric relaxations identified previously in neat PCL had to be added to the universal dynamic response, which describes ac electronic or ionic conduction in a wide variety of disordered solids, independent of the details of the disorder.[34] The variation of the ac conductivity with angular frequency at constant temperature can be described by

$$\sigma'(\omega) = \sigma_{dc} + B\omega^s \qquad (1)$$

where ω is the angular frequency, σ_{dc} is the conductivity measured here at the lowest frequency used in the experiment, B depends on temperature only, and the s exponent varies with ω and temperature between 0 and 1. Equation 1 has been frequently used to fit the experimental data, but it lacked of any supporting foundation.[35] Dyre and Schroeder[36] interpreted the universal ac properties of a wide range of ion- or electron-conducting disordered materials with models based on underlying percolation conduction when the local randomly varying mobilities span over several decades. What is remarkable in their results is that the predictions hold for such a variety of materials independent of the kind of existing disorder and the type of charge carriers. The model predicts exponents s between 0.7 and 1, the most frequent experimental value being 0.8, for disordered materials where the hopping of charge carriers is performed over barriers which are spatially randomly varying.[37]

In Figure 5 we have plotted the three electrical responses for the PCL/MWCNT 0.3 wt % nanocomposite, i.e., $\sigma'(\omega)$, $\varepsilon''(\omega)$, $M''(\omega)$. The first approach was to fit the experimental data for $\sigma'(\omega)$ to eq 1, i.e., considering only the dc and ac contributions. The parameters obtained for the best-fit were $\sigma_{dc} = (2.07 \pm 0.01) \times 10^{-7}$ S/cm, $B = (3.0 \pm 0.2) \times 10^{-12}$ S/cm, and $s = 0.905 \pm 0.004$. The agreement with the conductivity data was excellent;

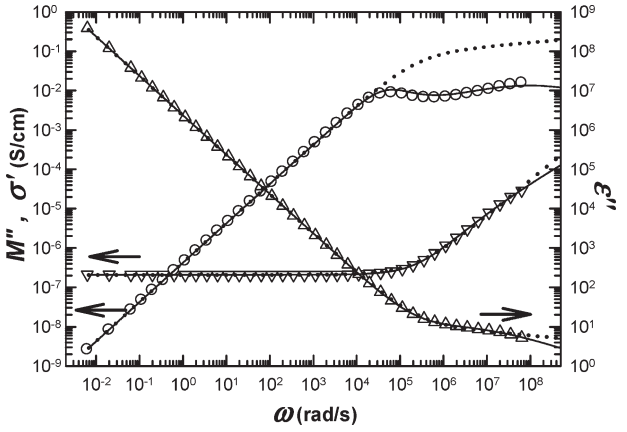

Figure 5. Analysis of the conductivity spectrum for PCL/MWCNT 0.3 wt % nanocomposite at room temperature: experimental data (∇), by fitting these experimental results to eq 1, dotted line. With these parameters, the dielectric loss (Δ) and electrical modulus (○) were simulated (dotted lines). The same procedure but the conductivity spectrum was now fitted with eq 2 and the simulations of $\varepsilon''(\omega)$ and $M''(\omega)$ are now plotted as continuous lines.

the dotted curve representing this fit is completely superimposed with the experimental points.

One way to ascertain the validity of our fitting in the conductivity representation is to simulate the response in the dielectric loss and electric modulus domain with the parameters given above obtained for the best fit of $\sigma'(\omega)$ to eq 1. The comparison of these simulations to the experimental data in the two other representations, $\varepsilon''(\omega)$ and $M''(\omega)$ data, is shown in Figure 5. These parameters allow an excellent fit of the dielectric loss, but did not reproduce the profile of the $M''(\omega)$ data at high frequencies (see the dotted curve). This discrepancy, observed only in the M'' formalism, led us to add the contribution of a dipolar relaxation mode with a Cole−Cole relaxation time distribution. The symmetric profile was chosen over the more general Havriliak−Negami one because of the semicrystalline character of PCL and the numerous demonstrations of its sufficiency to describe the relaxation time distribution of the dipolar species in the amorphous regions of a semicrystalline polymer.[38] A new fitting of the $\sigma'(\omega)$ data to eq 2 was then performed:

$$\sigma'(\omega,p) = \sigma_{dc} + B\omega^{s} + \frac{\omega\varepsilon_0\Delta\varepsilon(\omega\tau)^{\alpha}\sin(\pi\alpha/2)}{1+2(\omega\tau)^{\alpha}\cos(\pi\alpha/2)+(\omega\tau)^{2\alpha}} \quad (2)$$

As expected, the universal s exponent is the most sensitive to this addition and it changed from 0.905 to 0.8 when the Cole−Cole distribution is taken into account. The difference is significant only at high frequencies, as can be seen from the mean τ value. The new set of parameters given in Table 1 was then used to simulate $\varepsilon''(\omega)$ and $M''(\omega)$ data. In Figure 5 the continuous lines represent the simulation of the three functions with this second set of parameters, and one can observe the excellent agreement with the data in the three different formalisms. It is to be noted that in dielectric loss and conductivity domains the difference between the dotted and continuous curves is not visible. From the similarity of the mean relaxation time of the Cole−Cole mode added here and the values found for neat PCL[33] at room temperature for the αβ peak, one can conclude

Table 1. Parameters Obtained for PCL/CNT 0.3% from the Best Fit of $\sigma'(\omega)$ Data at Room Temperature to eq 2

αβ mode		UDR parameters	
α_{CC}	0.42 ± 0.04	σ_{dc} (S/cm)	$(2.095 \pm 0.002) \times 10^{-7}$
τ_{CC} (s)	$(4.3 \pm 0.8) \times 10^{-7}$	B (S/cm)	$(5 \pm 6) \times 10^{-12}$
$\Delta\varepsilon_{CC}$	42 ± 10	s	0.8 ± 0.1

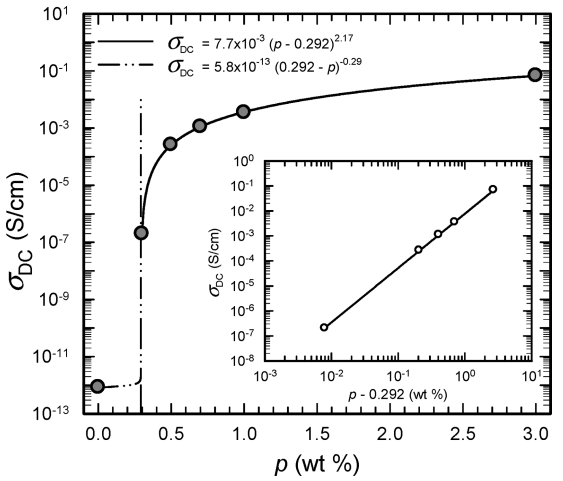

Figure 6. Dc conductivity of PCL/MWCNT composites as a function of the weight percent concentration of the nanofiller. The symbols are the data at room temperature, and the lines the fitting to eqs 3 and 4. The inset shows the linear dependence of $\log(\sigma_{dc})$ with $\log(p - p_c)$.

that when a relaxation mode is comprised in the frequency range explored, at least at low CNT concentrations, the analysis must include this contribution; otherwise, the exponents determined are only apparent but not appropriate for the description of the three functions simultaneously. Thus, the utility of finding a unique set of parameters for the fit in the three representations led to the inclusion of a feature that was not evident in the conductivity variation alone. In our case, the fit of the $M''(\omega)$ data was the most sensitive to the contribution of this mode. Previously, it has been demonstrated that the electric modulus representation is sometimes useful to minimize the effect of the dc conductivity in insulating materials, which sometimes hid important features of the dielectric loss spectrum.[39] Sidebottom et al.[40] compared the electric modulus formalism to the conductivity representation in ion conducting solids. They concluded that $M''(\omega)$ is not a suitable tool to provide comparative analysis due to the inclusion of a sensitive parameter, as the value of ε_∞ is. It is to be noted that in our case, before including the relaxation mode, we tried to vary the ε_∞ value alone to model the shape of our data in the modulus representation without success. As a conclusion, we can say that in the determination of the best parameters for modeling the conductivity data, the shape of the modulus curve guided us to a better set than those obtained by the Jonscher equation only.

3.3. Dc Electrical Conductivity Analysis. One important parameter for potential applications of these composites is the value of the percolation threshold, p_c, i.e., the CNT weight percent concentration sufficient to form the infinite cluster or conductive path through the sample. The plot represented in Figure 6 of $\log(\sigma_{dc})$ vs p shows the steep increase of the conductivity with the CNT concentration in the

nanocomposites. The precise determination of p_c is made through the fitting of the data to the scaling law:

$$\sigma_{dc}(p) = \sigma_0(p - p_c)^t \qquad \text{for } p > p_c \qquad (3)$$

$$\sigma_{dc}(p) = \sigma_0(p_c - p)^{-s'} \qquad \text{for } p < p_c \qquad (4)$$

The critical concentration was found to be p_c = 0.292% ± 0.005% and the critical exponent is t = 2.17 ± 0.02 for the PCL/CNT nanocomposites. The universal value calculated by Monte Carlo simulations for the critical exponent t is 2.0 in the case of a 3D percolation network,[26,41] which is close to the value found here. This electrical percolation threshold compared to previous determinations after rheological experiments on PCL/MWCNT (p_c = 2%−3%)[15,22] is quite low and suggests a good dispersion of the CNT in the polymer matrix. When the MWCNT were purified by HNO_3 treatment, which opens their end-capsule, the percolation threshold at room temperature, as determined by the variation of dc conductivity, increased from 2 to about 4 wt %;[22] both values are significantly higher than the value of 0.3 wt % determined here. In the case of the PCL/PLA/CNT nanocomposites,[19] we found a higher p_c value, 0.98%, which was to be expected, as part of the carboxylic nanotubes were found to be selectively located around the PLA inclusions, thus not contributing to the formation of the infinite cluster. If this segregation had not occurred, the percolation threshold should diminish as the CNT exclusion from the regions occupied by the PLA inclusions, amounting to 30 wt % of the sample, would increase the effective concentration of the nanofiller in the PCL phase. This difference between PCL and PCL/PLA should be higher in the case of pristine CNT, as the functionalization increases the conductivity by 4 orders of magnitude in the ternary compounds. A previous determination of these parameters for PCL/SWCNT composites from dc conductivity results was performed by Mitchell and Krishnamoorti[16] with different final results, i.e. t = 1.5 ± 0.2 and $p_c \sim$ 0.08%. In that case, the percolative lattice was found to be 2D, as the corresponding predicted values range from 1.10[42] to 1.43.[43] The lower dimensionality is attributed to thermally induced hopping between the loosely bound components of the infinite cluster. The low critical concentration obtained demonstrates that the use of a zwitterionic surfactant lead to an excellent dispersion of the SWCNT.

Another test for the CNT dispersion is to calculate the aspect ratio, L/R, of the nanofiller from the relation of the average excluded volume and the percolation onset. Balberg et al.[44,45] assumed that if the particles are randomly oriented sticks of length L and radius $R = W/2$ and if their critical particle concentration per unit volume is N_c, then the following relation can be written: $N_c 2WL^2(\pi/4) \approx 1.4$. In our nanocomposites the estimated value of L/R would be ∼1000. This number should be compared to the mean value given by Nanocyl, which is 150, calculated with the mean length of the CNT. However, these MWCNT are characterized by a very large distribution in size, as some of the CNT are even longer than 10 μm, as measured by transmission electron microscopy.[46] The observed difference indicates that the CNT are arranged in long stick bundles randomly distributed in the PCL matrix. This high estimated value for L/R is indicative of the absence of fracture of the CNT during the melt mixing in the miniextruder. The low value of p_c as compared to other determinations indicates the good nanofiller dispersion and explains the agreement found between our results and the predictions of the percolation theory in this system.

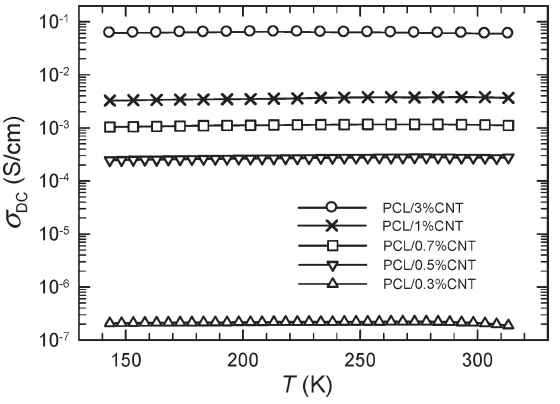

Figure 7. Variation of σ_{dc} with temperature for the PCL/MWCNT nanocomposites.

3.4. Variation of Dc Conductivity with Temperature. The data was collected in a wide temperature range, from 133 to 313 K, which is still below the melting temperature of the PCL crystallites. As the glass transition of PCL is T_g = 207 K, the amorphous regions of the semicrystalline PCL are first glassy and above T_g change to a rubbery state during our measurements. In the lower temperature range, the chain mobility is reduced to local motions whereas, for $T > T_g$, the CNT are surrounded by PCL chains moving in a cooperative way.

In Figure 7 we have represented the variation of σ_{dc} with temperature for $p \geq p_c$. The independence of the dc conductivity values with temperature is shown for all p values. This suggests that the onset of the cooperative motion of the polymeric chains above T_g does not affect the conductivity appreciably. Neither the critical exponent, t, nor the percolation threshold, p_c, vary significantly within the temperature range 133 K ≤ T ≤ 313 K. However, on passing through the glass transition temperature, a very small step decrease (2%) in the t value was found, while the p_c value increased simultaneously (0.3%) when the matrix became rubbery. These variations are well within the experimental errors but larger than the statistical errors of each determination. These clear tiny steps near T_g might be indicative of changes in the polymer matrix and may be associated to the onset of the segmental mobility and to the steep increase in the expansion coefficient of the rubbery phase as compared to the glassy states. The tiny but steep jumps observed at $T \sim T_g$ might be explained as the manifestation of the glass transition in conductivity domain when the infinite cluster formation is retarded by the extra nanotubes separation.

The almost constant value of σ_{dc} over the whole temperature range for each p value shown in Figure 7 has not been found in other systems, such as polyepoxy/MWCNT,[25] poly(butylene terephtalate)/MWCNT,[47] poly(ethylene terephtalate)/carbon black,[48] or poly(vinyl chloride)/carbon spheres aggregates.[49] In the three first nanocomposites, a σ_{dc} variation over near one decade is reported for each concentration, i.e., a temperature-activated process, which is not the case in our nanocomposites. For the PVC-based composites the temperature dependence is much higher. The contribution of conduction by charge carriers tunneling through the thin barriers formed by the polymer chains in which the CNT are embedded has been demonstrated to exist in these nanocomposites. Then, the variation of the dc

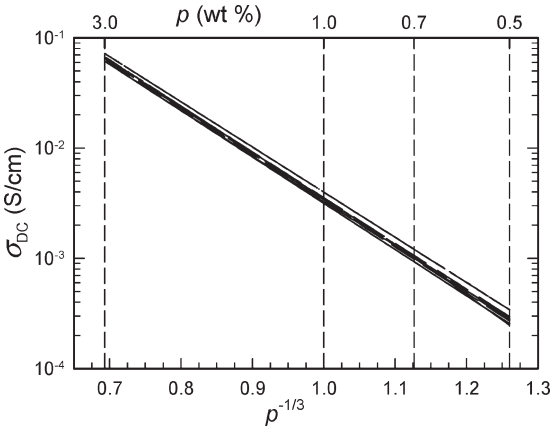

Figure 8. Electrical dc conductivity of PCL/MWCNT composites vs $p^{-1/3}$ for temperatures ranging from 133 to 313 K and 0.5 wt % $\leq p \leq$ 3 wt %.

conductivity should depend on the distance among the CNT not yet in physical contact. In the first approximation, the insulating gaps should then vary linearly as $p^{-1/3}$, which is proportional to the volume fraction $\varphi^{-1/3}$; the dc conductivity should then decrease exponentially with $p^{-1/3}$, and this relationship is illustrated in Figure 8, where we have plotted $\log(\sigma_{dc})$ as a function of $p^{-1/3}$, for $p \geq 0.5\%$ at different temperatures. The lines are the linear regression for the different p values at each temperature from 133 to 313 K by 10 K steps.

The almost perfect superposition observed among the isotherms plotted in Figure 8 indicates the existence of *conventional tunneling conduction* through insulating potential barriers between the CNT, as it is independent of temperature. With great differences in morphology and CNT dispersion, close results were observed in the ternary PCL/PLA/CNT nanocomposites.[19] In other nanocomposites, this dependence exists but varies with temperature, and it has been necessary to use the fluctuation-induced tunneling, TFIT, model introduced by Sheng[50] to explain the variation observed in the $\log(\sigma_{dc})$ vs $p^{-1/3}$ as the temperature changes. The model provides the following expression for the temperature variation of σ_{dc} for a given CNT concentration:

$$\sigma_{dc}(T) = \sigma_0\left(-\frac{T_1}{T+T_0}\right) \tag{5}$$

The T_0 parameter is interpreted as a limit temperature; above T_0 the fluctuations have to be considered. T_1 is related to the shape of the energy barrier through which tunneling takes place. In the case of polyethylene terephtalate/carbon black nanocomposites, the TFIT model describes the data above 45 K, and for lower temperatures, the conventional tunneling conductive process is valid. For the PVC nanocomposites, the nanofiller being in that work carbon spheres aggregates, the very low temperature conductivity varies according to the TFIT model.[49] Nogales et al.[47] also found a reasonable agreement of the experimental data with the model. On the other hand, for the nanocomposites polyepoxy/CNT, Barrau et al.[25] found a significant variation in $\log(\sigma_{dc})$ vs $p^{-1/3}$ within the temperature range used, but their results did not fit the TFIT model accurately. The temperature-independent behavior of σ_{dc} in the PCL/CNT nanocomposites simplifies the interpretation, as the conventional tunneling model is valid here over a wide temperature range (133−313 K).

3.5. Critical Exponents from Ac Conductivity. Bergman and Imry[51] simulation results showed that the variation with angular frequency in the percolation concentration vicinity of the ac conductivity and dielectric constant of a heterogeneous mixture might be described by a power law:

$$\sigma(\omega, p_c) \propto \omega^x \tag{6}$$

$$\varepsilon(\omega, p_c) \propto \omega^{-y} \tag{7}$$

the scaling relation being $x + y = 1$. It is to be noted that the exponent x is equal to s in the Jonscher equation (see eq 1). These authors report a value of $x = 0.73$ after numerical simulations of random resistors network. The frequency dependence of these functions has been attributed to the polarization effects between clusters in the matrix,[52] and the relation between x and y with the critical exponents t and s' (eq 3 and 4) is found to be

$$x = \frac{t}{t+s'} \qquad y = \frac{s'}{t+s'} \tag{8}$$

In this work, the exponents x and y were determined from the slopes of the conductivity and dielectric loss data corresponding to the nanocomposites with 0.3% CNT in Figure 3a,b. The values of $x = 0.8$ and $y = 0.24$ (after subtracting the contribution of the dielectric $\alpha\beta$ relaxation from the high-frequency slope) were determined, and the value for the sum $x + y = 1.04$ is close to the scaling relation. However, this small difference causes the calculated values of s' after eq 8 to differ by 20%.

Another model based on anomalous diffusion within each percolating cluster was proposed by Gefen et al.[53] If only the anomalous diffusion is considered, the x and y exponents can be related to the critical exponent t by the following expressions

$$x = \frac{t}{\nu(2+\theta)} \qquad y = \frac{2\nu-\beta}{\nu(2+\theta)} \tag{9}$$

where $\theta = 1.5$, $\beta = 0.5$, and $\nu \approx 0.9$ for 3D clusters. In this model, y is independent of t and x is proportional to t. For the PCL/CNT composites, $x = 0.8$ and $y = 0.41$, if calculated by means of eq 9. These values disagree with the general scaling relation. Comparing our results for the intercluster polarization and the anomalous diffusion we can conclude that the values found for the PCL/MWCNT composites are closer to the predictions of the intercluster polarization model. The intercluster polarization was also shown to predict values closer to the experimental results obtained by Song et al.[54] in a mixture of carbon and Teflon powder.

3.6. Characteristic Frequencies. As the frequency increases above the critical frequency, ω_c, the ac conductivity increases steeply, as can be seen for the three lower concentrations in Figure 3a. For higher concentrations, ω_c is out of our frequency window (10^{-3} Hz $\leq f \leq 10^7$ Hz). The scaling law between the characteristic frequency ω_c and the reduced mass fraction, $p - p_c$, is written as

$$\omega_c \propto (p - p_c)^{\nu/a} \tag{10}$$

which is derived from the scaling law between the correlation length, ξ (related to the mean distance between the percolative lattice points), and the concentration, assuming that ω_c is associated with ω_ξ, which is the angular frequency corresponding

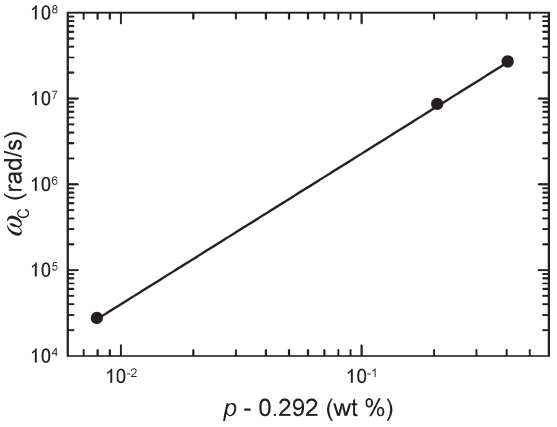

Figure 9. Concentration dependence of the critical frequency. The exponent obtained from the linear regression is $\nu/a = 1.694 \pm 0.001$.

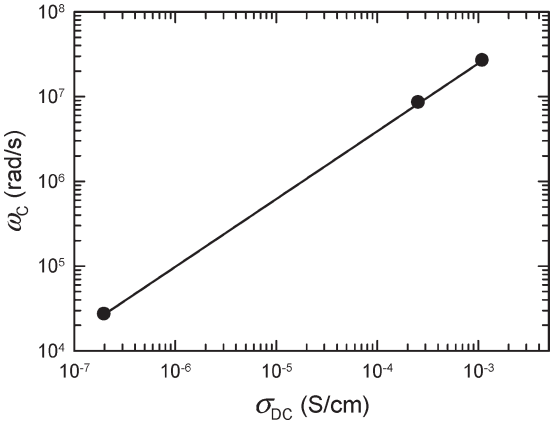

Figure 10. Conductivity dependence of the critical angular frequency of PCL/MWCNT for 0.3 wt % $\leq p \leq$ 0.7 wt %. Exponent obtained from the linear regression is $\nu/at = 0.780 \pm 0.001$.

to a distance traveled by the charge carriers equal to ξ. Then, one can write

$$\xi \propto (p - p_c)^{-\nu} \tag{11}$$

The value of ν depends on the dimensionality of the percolative lattice, and for 3D it has been estimated as somewhat smaller than 0.9.[26] A relation between the critical frequency and the distance ξ will depend on the randomness of the trajectory of the charge carriers in the walk. The walk could be completely random ($a = 0.5$) or biased ($0.5 \leq a < 1$) in the presence of high electric fields.[55]

By combining eqs 3 and 10, a relationship between ω_c and σ_{dc} can be expressed as

$$\omega_c \propto \sigma_{dc}^{\nu/at} \tag{12}$$

In Figures 9 and 10 we have represented the log−log plots of the critical frequency variation vs the reduced concentration or the σ_{dc} corresponding values, respectively. From the slopes of the regression line we obtained $\nu/a = 1.694 \pm 0.001$ and $\nu/at = 0.780 \pm 0.001$. If the value previously determined for t ($t = 2.17$) and $\nu_{3D} = 0.9$ are used, then $a = 0.53$, which is within the interval 0.5−1 predicted for this parameter and shows that the walk is nearly random.

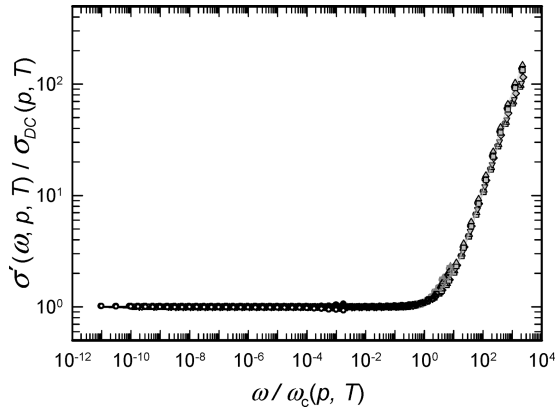

Figure 11. Master curve describing the variation of normalized ac conductivity as a function of normalized frequency of PCL/CNT composites, for 0.3 wt % $\leq p \leq$ 4 wt % and 133 K $\leq T \leq$ 313 K.

3.7. Master Curves. The universality of the ac conductive process in various and numerous disordered materials has been shown to exist. Time−concentration superposition has been demonstrated in several percolative systems for $p \geq p_c$.[19,25,48,55] This feature implies that the profile of $\log(\sigma')$ vs $\log(\omega)$ is common to all the nanocomposites with nanofiller concentrations above the percolation threshold and thus they can be superimposed by normalizing the variables plotted. It has also been claimed by Wu et al.[15] that the time−temperature superposition may not exist in the PCL/MWCNT system, at least when applying it to rheological data (Han plots) in the range of 343−368 K, i.e., in a molten state, due to changes in the percolative lattice. In the case of the electrical percolation in the PCL/CNT studied here, in order to draw a master curve which will show time−temperature−CNT concentration superposition, the conductivity curves were normalized, $\log[\sigma'(\omega,T,p)/\sigma_{dc}(T,p)]$ vs $\log[\omega/\omega_c(p)]$ for each composite ($p \geq p_c$) at various temperatures (133 K < T < 314 K, by 20 K steps). Time−temperature−CNT concentration superposition in this case is observed, as seen in Figure 11, where all the normalized curves at different temperatures below the melting point of PCL, for all the CNT concentrations of the nanocomposites, collapse in a single master curve, which extends from 10^{-11} to 10^4 Hz, i.e., in a much wider frequency range than the frequency window available in our experiments. As ω_c was not measurable for high CNT contents in the frequency window explored in this work, its value for drawing the master curve shown in Figure 11 was found by extrapolation of the $\omega_c$vs σ_{dc} curve plotted in Figure 10. The master curve obtained in this way describes the ac conductivity variation with frequency for all nanocomposite compositions and temperatures. The slope of the plot in Figure 11 for $\omega > \omega_c$ is 0.78, which could be interpreted as the average value for the apparent s exponent (eq 1) at all temperatures and compositions for the PCL/MWCNT composites. If we recall the presence at room temperature of the $\alpha\beta$ dipolar relaxation mode, which had to be taken into account when extracting the true s exponent from the conductivity plots, $s = 0.8$, this contribution is steeply variable with temperature. The relaxation mode sweeps our frequency window as the temperature increases and overlaps the conductivity rise only around room temperature. Therefore, the mean value $s = 0.78$ is a better choice, as it includes a wide composition and temperature variation. The Dyre's model[37] predicted value for this exponent is 0.8, which is frequently

found in the literature. In the PCL/PLA/CNT nanocomposites a time concentration superposition was only found and the Taylor−Isard scaling had to be applied, i.e. σ/σ_{dc} vs $\omega/\sigma_{dc}T$.[19] This corresponds to a different universality class; as in neat PCL nanocomposites, a perfect time−temperature−composition superposition after a simple normalization was found.

The existence of time−temperature−composition superposition demonstrated here for our electrical results in PCL/MWCNT was not found in the previous study of PCL/SWCNT by Mitchell and Krishnamoorti[16] for their melt rheology results, where the percolative cluster was 2D.

4. CONCLUSIONS

We have carried out a complete dc and ac conductivity, dielectric loss, and electric modulus characterization in wide frequency and temperature ranges of nanocomposites based on insulating, semicrystalline PCL, which complements previous rheological[15,16,22] and morphological[17,20] characterization with the determination of UDR parameters, percolation critical exponents, and universality. Additionally, the temperature range explored here corresponds to PCL amorphous regions either in the vitreous or the rubbery state. Several conclusions might be drawn:

(a) The dc conductivity is characteristic of a 3D percolative cluster with a low percolation threshold, p_c = 0.292 wt %, and a critical exponent t = 2.17 at room temperature. Over the wide temperature range studied here (133−313 K), p_c was determined, and its variation with temperature is found to be within the experimental error; however, around the glass transition temperature a clear but very weak jump is present. Simultaneously $t(T)$ is also a step function with a jump to lower values around T_g. The variation of t is within 2% in the whole temperature range.

(b) The frequency dependence of the conductivity of the nanocomposites can be described by the UDR characteristic of hopping conduction in disordered solids, but around room temperature a Cole−Cole mode had to be added in order to fit the electrical response in the three representations, σ', ε'', M''. When extracting the s exponent care has to be taken to consider all the possible contributions in order to find a true s exponent at low p values. A master curve which shows time−temperature−concentration superposition is obtained when the conductivity and angular frequency data are scaled, $\sigma'(\omega,p,T)/\sigma_{dc}(p,T)$ and $\omega/\omega_c(p,T)$, and the variables plotted in a log−log graph. The curve describes, in an extended frequency range, the conductivity at all temperatures and for concentrations above p_c. The s exponent extracted from the master curve, which is an average over concentration and temperature, is 0.78, in agreement with predictions of hopping conductivity model.

(c) Among the models available to describe the variation of $\sigma(\omega)$, $p > p_c$, the relation between the critical exponents of the scaling equation, x and y, the predictions of the intercluster polarization are nearly followed if the average s value extracted from the master curve is used. The anomalous diffusion model inside the clusters is not predictive of our results, as y has a constant value of 0.42, which is far from our experimental result.

(d) The parameters that characterize best the scaling laws of ω_c and σ_{dc} as a function of $(p - p_c)$ confirm the 3D character of the infinite cluster with t = 2.17 and a = 0.53, which indicates a 3D almost random walk.

(e) The invariance of the σ_{dc} over the wide temperature interval, which comprises sub- and super-T_g temperatures, is not a common feature of the reported data on polymer-based nanocomposites. The few works which report variable temperature studies show variations that are about one decade in the log $\sigma_{dc}(T)$ plot, and this variation has been explained in some cases by Sheng's model of tunneling conduction with thermally activated fluctuating energy barriers with different degrees of agreement. The similarity of the variation of $\sigma_{dc}(p^{-1/3})$ with T found here indicates that we are in the presence of a conventional tunnel effect, i.e., independent of temperature.

(f) In our previous work on the ternary nanocomposite PCL/PLA/carboxylic MWCNT, the nanofiller was dispersed in the PCL phase only and selectively on the interface of the PLA inclusions of the sea-island morphology of the material. The larger aspect ratio of the CNT bundles in the PCL-based nanocomposites agrees with a much lower p_c value. In spite of the huge differences between both systems (CNT functionalization, morphology and CNT distribution), some similarities were found in the critical exponents cluster dimensionality and the conventional tunnel effect conduction. However, the extracted parameter values are in better agreement with the expected values for neat PCL than the blend nanocomposites.

AUTHOR INFORMATION

Corresponding Author

*E-mail: elaredo@usb.ve. Tel: +58-212-906-3536. Fax: +58-212-906-3527.

ACKNOWLEDGMENT

We are grateful to the following funding agencies for the support of this work: for the Venezuelan groups to FONACIT (Projects F2005-000284 and G2005-000776), and to USB (DID-G15 and G-02); CIRMAP thanks the "Belgian Federal Government Office Policy of Science (SSTC)" for general support in the frame of the PAI-6/27. The collaboration of M. A. Mujica for the DSC experiments was greatly appreciated.

REFERENCES

(1) Paul, D. R.; Robeson, L. M. *Polymer* **2008**, *49*, 3187–3204.
(2) Endo, M.; Strano, M. S.; Ajayan, P. M. In *Carbon Nanotubes Advanced Topics in the Synthesis, Structure, Properties and Applications*; Jorio, A., Dresselhaus, G., Dresselhaus, M. S., Eds.; Springer; Berlin, 2008; pp 13−62.
(3) Geng, J.; Zeng, T. *J. Am. Chem. Soc.* **2006**, *128*, 16827–16833.
(4) Arranz-Andrés, J.; Blau, W. J. *Carbon* **2008**, *46*, 2067–2075.
(5) Li, C.; Thostenson, E. T.; Chou, T. W. *Compos. Sci. Technol.* **2008**, *68*, 1227–1249.
(6) Du, F.; Scogna, R. C.; Zhou, W.; Stijn, B.; Fischer, J. E.; Winey, K. I. *Macromolecules* **2004**, *37*, 9048–9055.
(7) Sahoo, N. G.; Rana, S.; Cho, J. W.; Li, L.; Chan, S. H. *Prog. Polym. Sci.* **2010**, *35*, 837–867.
(8) Moniruzzaman, M.; Winey, K. I. *Macromolecules* **2006**, *39*, 5194–5205.
(9) Bauhofer, W.; Kovacs, J. Z. *Compos. Sci. Technol.* **2009**, *69*, 1486–1498.

(10) Logakis, E.; Pandis, Ch.; Peoglos, V.; Pissis, P.; Pionteck, J.; Pötschke, P.; Micusík, M.; Omastová, M. *Polymer* **2009**, *50*, 5103–5111.
(11) Newman, D.; Laredo, E.; Bello, A.; Grillo, A.; Feijoo, J. L.; Müller, A. J. *Macromolecules* **2009**, *42*, 5219–5225.
(12) Wu, D.; Zhang, Y.; Zhang, M.; Zhou, W. *Eur. Polym. J.* **2008**, *44*, 2171–2183.
(13) Laredo, E.; Prutsky, N.; Bello, A.; Grimau, M.; Castillo, R. V.; Müller, A. J.; Dubois, Ph. *Eur. Phys. J. E* **2007**, *23*, 295–303.
(14) Krishnamoorti, R.; Giannelis, E. P. *Macromolecules* **1997**, *30*, 4097–4102.
(15) Wu, D.; Wu, L.; Sun, Y.; Zhang, M. *J. Polym. Sci. Part B: Polym. Phys.* **2007**, *46*, 3137–3147.
(16) Mitchell, C. A.; Krishnamoorti, R. *Macromolecules* **2007**, *40*, 1538–1545.
(17) Chen, E.-C.; Wu, T.-M. *Polym. Degrad. Stab.* **2007**, *92*, 1009–1015.
(18) Wu, D.; Zhang, Y.; Zhang, M.; Yu, W. *Biomacromolecules* **2009**, *10*, 417–424.
(19) Laredo, E.; Grimau, M.; Bello, A.; Wu, D. F.; Zhang, Y. S.; Lin, D. P. *Biomacromolecules* **2010**, *11*, 1339–1347.
(20) Mitchell, C. A.; Krishnamoorti, R. *Polymer* **2005**, *46*, 8796–8804.
(21) Spitalsky, Z.; Tasis, D.; Papagelis, K.; Galiotis, C. *Prog. Polym. Sci.* **2010**, *35*, 357–401.
(22) Saeed, K.; Park, S. Y. *J. Appl. Polym. Sci.* **2007**, *104*, 1957–1963.
(23) Pötschke, P.; Dudkin, S. M.; Alig, I. *Polymer* **2003**, *44*, 5023–5030.
(24) Linares, A.; Canalda, J. C.; Cagiao, M. E.; García-Gutierrez, M. C.; Nogales, A.; Martín- Gullón, I.; Vera, J.; Ezquerra, T. A. *Macromolecules* **2008**, *41*, 7090–7097.
(25) Barrau, S.; Demont, Ph.; Peigney, A.; Laurent, C.; Lacabanne, C. *Macromolecules* **2003**, *36*, 5187–5194.
(26) Stauffer, D.; Aharony, A. *Introduction to Percolation Theory*; Taylor and Francis: London, 2003.
(27) Bittiger, H.; Marchessault, R. H.; Niegisch, W. D. *Acta Crystallogr. B* **1970**, *26*, 1923–1927.
(28) Schultz, J. M. In *Polymer Crystallization, the Development of Crystalline Order in Thermoplastic Polymers*: Oxford University Press: Washington, DC, 2001.
(29) Wu, T.-M.; Chen, E.-C. *Polym. Eng. Sci.* **2006**, *46*, 1309–1317.
(30) Xu, G.; Du, L.; Wang, H.; Xia, R.; Meng, X.; Zhu, Q. *Polym. Internat.* **2008**, *57*, 1052–1066.
(31) Priftis, B.; Sakellariou, G.; Hadjichristidis, N.; Penott-Chang, E.; Lorenzo, A. T.; Müller, A. J. *J. Polym. Sci., Part A: Polym. Chem.* **2009**, *47*, 4379–4390.
(32) Müller, A. J.; Arnal, M. L.; Trujillo, M.; Lorenzo, A. T. *Eur. Polym. J.* **2011**in press (DOI: 10.1016/j.europolymj.2010.09.027).
(33) Grimau, M.; Laredo, E.; Perez, Y. M. C.; Bello, A. *J. Chem. Phys.* **2001**, *114*, 6417–6425.
(34) Jonscher, A. K. *Nature* **1977**, *267*, 673–679.
(35) Schönhals, A.; Kremer, F. In *Broadband Dielectric Spectroscopy*; Kremer, F., Schönhals, A., Eds.; Springer: Berlin, 2003; pp 59−98 .
(36) Dyre, J. C.; Schroder, T. B. *Rev. Mod. Phys.* **2000**, *72*, 873–892.
(37) Dyre, J. C. *J. Appl. Phys.* **1988**, *64*, 2456–2468.
(38) Laredo, E.; Grimau, M.; Barriola, P.; Bello, A.; Müller, A. *Polymer* **2005**, *46*, 6532–6542.
(39) Bello, A.; Laredo, E.; Grimau, M. *J. Non-Cryst. Solids* **2007**, *353*, 4283–4287.
(40) Sidebottom, D. L.; Roling, B.; Funke, K. *Phys. Rev. B* **2000**, *63*, 024301–7.
(41) Sahimi, M. *Applications of Percolation Theory*; Taylor and Francis: London, 1993.
(42) Straley, J. P. *Phys. Rev. B* **1977**, *15*, 5733–5737.
(43) Fisch, R.; Harris, A. B. *Phys. Rev. B* **1978**, *18*, 416–420.
(44) Balberg, I.; Anderson, C. H.; Alexander, S.; Wagner, N. *Phys. Rev. B* **1984**, *30*, 3933–3943.
(45) Balberg, I.; Binenbaum, N.; Wagner, N. *Phys. Rev. Lett.* **1984**, *52*, 1465–1468.
(46) Nanocyl, private communication.
(47) Nogales, A.; Broza, G.; Roslaniec, Z.; Sics, I.; Hsiao, B. S.; Sanz, A.; Garcia-Gutierrez, M. C.; Rueda, D. R.; Domingo, C.; Ezquerra, T. A. *Macromolecules* **2004**, *37*, 7669–7672.
(48) Connor, M. T.; Roy, S.; Ezquerra, T. A.; Baltá-Calleja, F. J. *Phys. Rev. B* **1998**, *57*, 2286–2294.
(49) Sheng, P.; Sichel, E. K.; Gittelman, J. L. *Phys. Rev. Lett.* **1978**, *40*, 1197–1200.
(50) Sheng, P. *Phys. Rev. B* **1980**, *21*, 2180–2195.
(51) Bergman, D. J.; Imry, Y. *Phys. Rev. Lett.* **1977**, *39*, 1222–1225.
(52) Webman, I.; Jortner, J.; Cohen, M. H. *Phys. Rev. B* **1977**, *16*, 2593–2596.
(53) Gefen, Y.; Aharony, A. *Phys. Rev. Lett.* **1983**, *50*, 77–80.
(54) Song, Y.; Noh, T. W.; Lee, S.-I.; Gaines, J. R. *Phys. Rev. B* **1986**, *33*, 904–908.
(55) Kilbride, B. E.; Coleman, J. N.; Fraysse, J.; Fournet, P.; Roth, S.; Blau, W. J. *J. Appl. Phys.* **2002**, *92*, 4024–4030.